Ultrafast holographic Stokesmeter for polarization imaging in real time

M. S. Shahriar, J. T. Shen, and Renu Tripathi

Department of Electrical and Computer Engineering, Northwestern University, Evanston, Illinois 60208

Mark Kleinschmit

Digital Optics Technologies, Incorporated, Somerville, Massachusetts 02144

Tsu-Wei Nee and Soe-Mie F. Nee

Research Department, Weapons Division, Naval Air Warfare Center, China Lake, California 93555-6100

We propose an ultrafast holographic Stokesmeter using a volume holographic substrate with two sets of two orthogonal gratings to identify all four Stokes parameters of the input beam. We derive the Mueller matrix of the proposed architecture and determine the constraints necessary for reconstructing the complete Stokes vector. The speed of this device is determined primarily by the channel spectral bandwidth (typically 100 GHz), corresponding to a few picoseconds. This device could be useful in high-speed polarization imaging. © 2004 Optical Society of America

OCIS codes: 090.0090, 050.7330, 120.5410.

Polarimetric imaging[1-3] takes advantage of the fact that a given object emits and scatters light in a unique way depending on its polarimetric signature. Identifying the polarimetric signature is equivalent to identifying the scattered Stokes vector.[4,5] An active polarimetric sensor is used in applications such as target recognition, vegetation mapping, pollution monitoring, geological surveys, and medical diagnostics.[6-9]

Current polorization imaging systems include mechanical quarter-wave plate–linear polarizer combinations,[10] photodetectors with polarization filtering gratings etched onto the pixels, and liquid-crystal variable retarders. The speed of the mechanical sensor is limited because each Stokes parameter is determined sequentially and the wave plate–polarizer combination must be reoriented precisely between parameters. The etched photodetector systems cannot resolve the complete Stokes vector at this time. The liquid-crystal retardation is similar to the mechanical sensor but with a liquid–crystal display replacing the wave plates and polarizers. This method is still sequential and is restricted by the time it takes the display to reorient itself, typically of the order of 100 ms/scan. This limits the throughput to ~10 Hz. To examine the advantages of the proposed architecture and to quantify its speed, we examine each component (see Fig. 1). A typical thick hologram (~1 mm) has a channel bandwidth of the order of 1 nm (and an angular bandwidth of ~1 mrad), corresponding to an optical response time of ~10 ps. The signal manipulation can be accomplished with precalibrated field-programmable gate arrays or programmable logic arrays and does not require real-time processing. These devices perform at approximtely the speed of the logic gates, typically of the order of 1 ns. The detector array response time is determined in part by the desired signal-to-noise ratio (SNR). The SNR is proportional to $\sqrt{\eta I \tau}$, where η is the quantum efficiency, I is the intensity, and τ is the average time. For a typical SNR of 10, the response time is then given by the detector-specific parameters and the amount of light reflected by the target. It should be noted that the constraints imposed by a given SNR and the detector array are common to all the methods discussed here. The advantage of our design is that it can determine the complete Stokes vector in parallel, so that the detector and not the sensor is the limiting factor in determining the speed of the device.

The architecture is shown in Fig. 1. The incoming image is split into two copies by use of a beam splitter. The first beam is diffracted into two beams by use of two multiplexed holographic gratings. The second beam passes through a quarter-wave plate before diffracting from a similar set of multiplexed holographic gratings. The diffracted beams are projected onto four CCD arrays. Their intensities are summed with predetermined weights to compute each component of the Stokes vector. These weighting factors are determined by use of the parallel and perpendicular polarization components of diffraction to formulate the Mueller matrix that describes the transformation of the initial Stokes parameters by grating diffraction. This design takes advantage of the fact
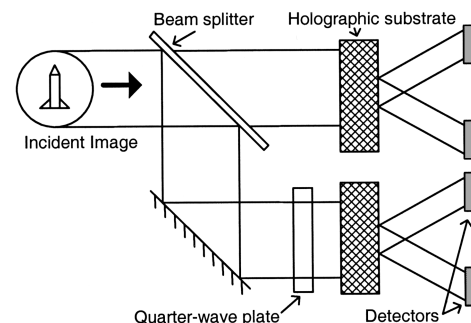

Fig. 1. Schematic of the holographic Stokesmeter.

© 2004 Optical Society of America

that a hologram is sensitive to the polarization of the incident light, and the weighting factors can be determined analytically by use of a Mueller matrix analysis of the architecture.

For an arbitrary image pattern the diffraction efficiencies also depend on the range of spatial frequencies. Here we restrict our analysis to the simple case of a plane wave incidence, which can be extended easily to analyze the general case. Figure 2 illustrates the progression of the light through a thick hologram. This process is represented mathematically by a series of Mueller matrices[11,12] that describe the transformation of the input Stokes vector $\mathbf{S}_i$. The Stokes vector $\mathbf{S}_{FS}$ of the transmitted beam through the front surface of the hologram is $\mathbf{S}_{FS} = \mathbf{M}_{FS}\mathbf{S}_i$, where $\mathbf{M}_{FS11} = \mathbf{M}_{FS22} = t_{\parallel}^2 + t_{\perp}^2$, $\mathbf{M}_{FS12} = \mathbf{M}_{FS21} = t_{\perp}^2 - t_{\parallel}^2$, and $\mathbf{M}_{FS33} = \mathbf{M}_{FS44} = 2t_{\parallel}t_{\perp}$. $\mathbf{M}_{FS}$ is the Mueller matrix for the transmission from the front surface and $t_{\parallel}$ and $t_{\perp}$ are the Fresnel transmission coefficients corresponding to the components of linearly polarized light parallel and perpendicular to the plane of incidence. One can describe the Mueller matrix for the exit surface of the hologram in the same manner.

To construct the Mueller matrix for the grating itself, $\mathbf{M}_H$ in Fig. 2, we describe the amplitude of the diffracted beam for parallel and perpendicular incidence in a manner analogous to the Fresnel reflection/transmission case. For our purposes here we need to describe only the diffracted beam and not the transmitted component. The relevant parameters are illustrated in Fig. 3: $\vec{U}_i$ is the input beam and $\vec{U}_o$ is the output beam, where $\hat{u}_i$ and $\hat{u}_o$ are the respective polarization vectors normal to the direction of propagation; $\mathbf{K}$ is the grating vector, which makes an angle ϕ with the z axis. We note that the amplitude of the diffracted beam is given by[13]

$$\frac{U_o}{U_i} = -i\alpha \, \sin\left(\left\{\frac{[\kappa(\hat{\mathbf{u}}_i \cdot \hat{\mathbf{u}}_o)d]^2}{\gamma}\right\}^{1/2}\right),$$

$$\alpha = \left(\frac{\cos\theta_i}{\cos\theta_o}\right)^{1/2}, \quad \gamma = \cos\theta_i \cos\theta_o, \quad \kappa = \pi n'/\lambda.$$

$$(1)$$

Here, n' is the index modulation depth. For the spectral cases of polarizations parallel and perpendicular to the plane of incidence, the dot product in Eqs. (1) can be simplified as

$$\frac{U_o}{U_i}(d)_{\perp} = u_{\perp} = -i\alpha \, \sin\left(\sqrt{\frac{\kappa^2 d^2}{\gamma}}\right),$$

$$\frac{U_o}{U_i}(d)_{\parallel} = u_{\parallel} = -i\alpha \, \sin\left\{\left[\frac{\kappa^2 \cos^2 2(\theta_i - \phi)d^2}{\gamma}\right]^{1/2}\right\}.$$

$$(2)$$

The Mueller matrix for the hologram ($\mathbf{M}_H$) and the transformation of the Stokes vector $\mathbf{S}_i$ are given by $\mathbf{S}_H = \mathbf{M}_H\mathbf{S}_i$, where $\mathbf{M}_{H11} = \mathbf{M}_{H22} = u_{\parallel}^2 + u_{\perp}^2$, $\mathbf{M}_{H12} = \mathbf{M}_{H21} = u_{\perp}^2 - u_{\parallel}^2$, and $\mathbf{M}_{H33} = \mathbf{M}_{H44} = 2u_{\parallel}u_{\perp}$.

For the architecture proposed above, we must describe the diffraction amplitudes from two multiplexed gratings. These gratings must be specifically designed so that they have the same Bragg angle θ_B. Following our previous analysis,[14] we can design two orthogonal gratings such that they each share the same Bragg angle. The amplitude of the diffracted beam from the jth grating is given as

$$\frac{U_o}{U_i}(d)_j = -i \, \frac{\kappa_j(\hat{\mathbf{u}}_i \cdot \hat{\mathbf{u}}_{oj})}{\cos(\theta_{oj})\xi_0} \sin(\xi_0 d) \quad \text{for } j = 1, 2,$$

where

$$\xi_0 = \left(\frac{1}{\cos(\theta_i)}\left\{\frac{[\kappa_1(\hat{\mathbf{u}}_i \cdot \hat{\mathbf{u}}_{o1})]^2}{\cos(\theta_{o1})} + \frac{[\kappa_2(\hat{\mathbf{u}}_i \cdot \hat{\mathbf{u}}_{o2})]^2}{\cos(\theta_{o2})}\right\}\right)^{1/2}.$$

$$(3)$$

We can evaluate the parallel and perpendicular polarization cases as in Eqs. (2) and obtain the proper coefficients $u_{\parallel}$ and $u_{\perp}$.

The proposed architecture can now be completely analyzed by use of the Mueller matrices found above. The Mueller matrix for one grating of the hologram is $\mathbf{M}_t = \mathbf{M}_{ES} \cdot \mathbf{M}_H \cdot \mathbf{M}_{FS}$ where $\mathbf{M}_{FS}$ is the matrix for the front surface and M_{ES} is the matrix for the exit surface. Using $\mathbf{M}_{ES}$, $\mathbf{M}_H$, and $\mathbf{M}_{FS}$, we find that the transformation of the input Stokes vector is given by $\mathbf{M}_{t11} = \mathbf{M}_{t22} = A + B$, $\mathbf{M}_{t12} = \mathbf{M}_{t21} = A - B$, and $\mathbf{M}_{t33} = \mathbf{M}_{t44} = 2\sqrt{AB}$, where $A = t_{FS\perp}^2 u_{\perp}^2 t_{ES\perp}^2$ and $B = t_{FS\parallel}^2 u_{\parallel}^2 t_{ES\parallel}^2$. This equation shows the Stokes vector that is diffracted from one grating. The second grating will produce an equation of the same form but with different grating coefficients u. Both equations have the same Stokes vector as input, but because grating parameters u differ, they will produce different output. Note that using intensity detectors, and
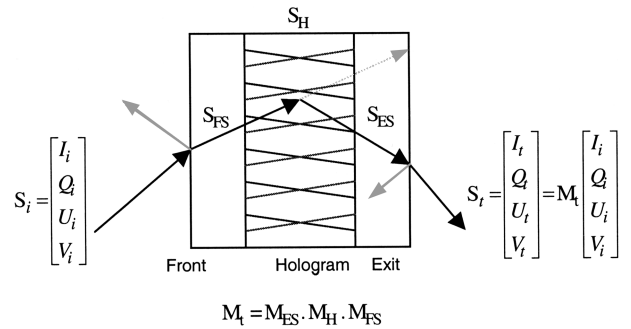
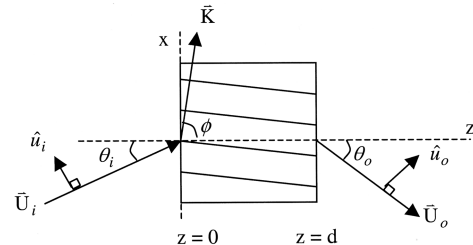Fig. 2. Interaction with the hologram viewed in three sections.

Fig. 3. Diffraction from a thick, slanted grating.

given the form of the Mueller matrix in the Stokes vector equation, we can determine only the first two Stokes parameters. To determine the other Stokes parameters, one must have a Mueller matrix with nonzero off-diagonal elements in the third and fourth columns. This can be achieved, for example, by a rotation of the holographic grating about the z axis and by a similar rotation of the polarization axis of the incident light. This rotation R_z is described by the following Mueller matrix:

$$\mathbf{M}_{R_z}(\gamma) = \begin{bmatrix} 1 & 0 & 0 & 0 \\ 0 & \cos 2\gamma & -\sin 2\gamma & 0 \\ 0 & \sin 2\gamma & \cos 2\gamma & 0 \\ 0 & 0 & 0 & 1 \end{bmatrix}. \quad (4)$$

This rotation allows us to find two equations for the two beams diffracted by the first set of multiplexed gratings:

$$I_{t1} = I_i(A_1 + B_1) + [Q_i \cos(2\gamma_1) - U_i \sin(2\gamma_1)]$$
$$\times (A_1 - B_1),$$
$$I_{t2} = I_i(A_2 + B_2) + [Q_i \cos(2\gamma_2) - U_i \sin(2\gamma_2)]$$
$$\times (A_2 - B_2), \quad (5)$$

where subscripts 1 and 2 denote the two separate gratings. Angle γ_1 denotes the angle of rotation for gratings 1 and 3. The next set of equations comes from the beams that pass through the quarter-wave plate and diffract from the third and fourth gratings. The quarter-wave plate adds a $\pi/2$ phase shift that interchanges the U and V parameters of the Stokes vector: $\cos(\epsilon) \rightarrow \cos(\epsilon + \pi/2) = -\sin(\epsilon)$ and $\sin(\epsilon) \rightarrow \sin(\epsilon + \pi/2) = \cos(\epsilon)$. The second set of equations is thus

$$I_{t3} = I_i(A_3 + B_3) + [Q_i \cos(2\gamma_1) + V_i \sin(2\gamma_1)]$$
$$\times (A_3 - B_3),$$
$$I_{t4} = I_i(A_4 + B_4) + [Q_i \cos(2\gamma_2) + V_i \sin(2\gamma_2)]$$
$$\times (A_4 - B_4). \quad (6)$$

Because the quarter-wave plate has changed U into V, we now have four equations that involve all four Stokes parameters. We are required to measure the four diffracted intensities to determine the Stokes parameters. Grating coefficients u and the Fresnel reflection coefficients can be measured to find the A and B coefficients, which in turn can be used to preweight the detector arrays for the imaging process.

To determine the constraints on the device parameters that are required to determine fully the complete Stokes vector, we write Eqs. (5) and (6) together in matrix form as $I_t = \mathbf{M}'S_i$, where $\mathbf{M}'$ is the so-called measurement matrix, S_i is the input Stokes vector to be solved for, and I_t represents the four measured intensities. For our material parameters, an example measurement matrix is given as

$$\mathbf{M}' = \begin{bmatrix} 0.24320 & -0.04187 & 0.23746 & 0 \\ 0.68596 & -0.03614 & 0.00637 & 0 \\ 0.28996 & -0.04897 & 0 & -0.27773 \\ 0.21291 & 0.11626 & 0 & 0.02050 \end{bmatrix}. \quad (7)$$

We have verified numerically that this matrix determines the Stokes vector robustly for a range of input values. No attempt was made to further optimize the condition[15,16] of the matrix, which requires an exhaustive search through the parameter space and is subject to further investigation.

We have proposed a polarization imaging architecture using thick multiplexed holograms that has many advantages over current polarimetric imaging techniques. The analysis showing the principle of operation explicitly takes into account the polarization state of the incident and diffracted wave fields. Transformation of initial Stokes parameters by grating diffraction is formulated by a Mueller matrix defined in terms of diffracted amplitudes of planar and perpendicular polarization components. A procedure has been outlined that uses two sets of rotated orthogonal gratings and a quarter-wave plate to compute all four unknown Stokes parameters required for polarimetric imaging.

References

1. J. L. Pezzaniti and R. A. Chipman, Opt. Eng. **34,** 1558 (1995).
2. K. P. Bishop, H. D. McIntire, M. P. Fetrow, and L. J. McMackin, Proc. SPIE **3699,** 49 (1999).
3. G. P. Nordin, J. T. Meier, P. C. Deguzman, and M. W. Jones, J. Opt. Soc. Am. A **16,** 1168 (1999).
4. W. S. Bickel and W. M. Bailey, Am. J. Phys. **53,** 468 (1985).
5. C. F. Bohren and D. R. Huffman, *Absorption and Scattering of Light by Small Particles* (Wiley, New York, 1998).
6. L. J. Denes, M. S. Gottlieb, B. Kaminsky, and D. F. Huber, Proc. SPIE **3240,** 8 (1998).
7. T. Nee and S. F. Nee, Proc. SPIE **2469,** 231 (1995).
8. W. G. Egan, Proc. SPIE **1747,** 2 (1992).
9. D. W. Beekman and J. V. Anda, Infrared Phys. Technol. **42,** 323 (2001).
10. D. Kim, C. Warde, K. Vaccaro, and C. Woods, Appl. Opt. **42,** 3756 (2003).
11. A. Gerrard and J. M. Burch, *Introduction to Matrix Methods for Optics* (Dover, New York, 1974).
12. S. F. Nee and T. W. Nee, Opt. Eng. **41,** 994 (2002).
13. H. Kogelnik, Bell Syst. Tech. J. **48,** 2909 (1969).
14. M. S. Shahriar, J. Riccobono, M. Kleinschmit, and J. T. Shen, Opt. Commun. **220,** 75 (2003).
15. A. Ambirajan and D. C. Look, Opt. Eng. **34,** 1651 (1995).
16. D. S. Sabatke, A. M. Locke, M. R. Descour, W. C. Sweatt, J. P. Garcia, E. L. Dereniak, S. A. Kemme, and G. S. Phipps, Proc. SPIE **4133,** 75 (2000).